

Article

Synthesis, Structural Studies, and Anticancer Properties of [CuBr(PPh₃)₂(4,6-Dimethyl-2-Thiopyrimidine-κS)]

Bandar A. Babgi ^{1,*}, Jalal H. Alsayari ¹, Bambar Davaasuren ², Abdul-Hamid Emwas ², Mariusz Jaremko ³, Magda H. Abdellatif ⁴ and Mostafa A. Hussien ^{1,5}

- ¹ Department of Chemistry, Faculty of Science, King Abdulaziz University, P.O. Box 80203, Jeddah 21589, Saudi Arabia; jalsayari@stu.kau.edu.sa (J.H.A.); mostafa_aly2@yahoo.com (M.A.H.)
- ² Core Labs, King Abdullah University of Science and Technology (KAUST), Thuwal 23955-6900, Saudi Arabia; bambar.davaasuren@kaust.edu.sa (B.D.); abdelhamid.emwas@kaust.edu.sa (A.-H.E.)
- ³ Biological and Environmental Science and Engineering (BESE), King Abdullah University of Science and Technology (KAUST), Thuwal 23955-6900, Saudi Arabia; mariusz.jaremko@kaust.edu.sa
- ⁴ Chemistry Department, Deanship of Scientific Research, College of Sciences, Taif University, Al-Haweiah, P.O. Box 11099, Taif 21944, Saudi Arabia; m.hasan@tu.edu.sa
- ⁵ Department of Chemistry, Faculty of Science, Port Said University, Port Said 42521, Egypt
- * Correspondence: bbabgi@kau.edu.sa

Abstract: CuBr(PPh₃)₂(4,6-dimethylpyrimidine-2-thione) (Cu-L) was synthesized by stirring CuBr(PPh₃)₃ and 4,6-dimethylpyrimidine-2-thione in dichloromethane. The crystal structure of Cu-L was obtained, and indicated that the complex adopts a distorted tetrahedral structure with several intramolecular hydrogen bonds. Moreover, a centrosymmetric dimer is formed by the intermolecular hydrogen bonding of the bromine acceptor created by symmetry operation 1-x, 1-y, 1-z to the methyl group (D₃ = C42) of the pyrimidine-thione ligand. HSA-binding of Cu-L and its ligand were evaluated, revealing that Cu-L binds to HSA differently than its ligand. The HSA-bindings were modeled by molecular docking, which suggested that Cu-L binds to the II A domain while L binds between the I B and II A domains. Anticancer activities toward OVCAR-3 and HeLa cell lines were tested and indicated the significance of the copper center in enhancing the cytotoxic effect; negligible toxicities for L and Cu-L were observed towards a non-cancer cell line. The current study highlights the potential of copper(I)-phosphine complexes containing thione ligands as therapeutic agents.

Keywords: copper(I); thiopyrimidine; phosphine; protein binding; anticancer properties



Citation: Babgi, B.A.; Alsayari, J.H.; Davaasuren, B.; Emwas, A.-H.; Jaremko, M.; Abdellatif, M.H.; Hussien, M.A. Synthesis, Structural Studies, and Anticancer Properties of [CuBr(PPh₃)₂(4,6-Dimethyl-2-Thiopyrimidine-κS)]. *Crystals* **2021**, *11*, 688. <https://doi.org/10.3390/cryst11060688>

Academic Editors: Assem Barakat and Alexander S. Novikov

Received: 17 May 2021
Accepted: 8 June 2021
Published: 16 June 2021

Publisher's Note: MDPI stays neutral with regard to jurisdictional claims in published maps and institutional affiliations.



Copyright: © 2021 by the authors. Licensee MDPI, Basel, Switzerland. This article is an open access article distributed under the terms and conditions of the Creative Commons Attribution (CC BY) license (<https://creativecommons.org/licenses/by/4.0/>).

1. Introduction

The coordination chemistry of N-heterocyclic-thiones with their tautomerization between the -NH-C(=S)- and -N=C(-SH)- forms was investigated with different transition metals, showing monomeric, dimeric, oligomeric, and polymeric complexes [1–3]. Specifically, the coordination chemistry of copper(I) has been widely investigated. One of the earliest studies was reported by Karagiannidis and co-workers, who reacted equimolar amounts of copper(I) halides and triphenylphosphine to produce [Cu(μ₃-I)(PPh₃)₄], which was subsequently treated with a range of pyridine-/pyrimidine-thiones [4]. The dimeric complexes [CuI(PPh₃)(μ-thione)]₂ were obtained and identified by single-crystal X-ray diffraction. In the same report, CuBr(PPh₃)₃ was stirred in THF with Zr(pyridine-2-thione)₄ to produce crystals of the monomeric complex [CuBr(PPh₃)₂(pyridine-thione-κS)] [4]. Setting the ratio of CuX to PPh₃ and thione at (1:2:1) produced complexes with CuX(PPh₃)₂(thione) [5–7]. In another report, tri(*p*-tolyl)phosphine was employed with CuCl and 1,3-thiazolidine-2-thione (equimolar ratio) for producing dimeric complexes with bridging thiones [8]. However, increasing the cone angle of the phosphine by employing tri(*m*-tolyl)phosphine produced dimeric complexes with either thiones or halides bridging ligands [9]. Further increase of the steric bulkiness by utilizing tri(*o*-tolyl)phosphine caused the formation of the trigonal planar copper(I) complex [CuX(P(*o*-tolyl)₃)(thione)] [10]. A series of mixed-ligand

mono- and dinuclear copper(I) halides with imidazolidine-2-thiones and triphenylphosphine were accessed by adopting a molar ratio of 1:2:1, producing three types of complexes: mononuclear tetrahedral $[\text{CuX}(\text{thione})(\text{PPh}_3)_2]$, halogen- and sulfur-bridged dimers, $[\text{Cu}(\mu\text{-Cl})(\kappa^1\text{-S-thione})(\text{PPh}_3)_2]$ and $[\text{CuI}(\mu\text{-S-thione})(\text{PPh}_3)_2]$ [11]. A range of bisphosphines were employed as co-ligands to access monomeric complexes with the general formula $[\text{CuX}(\text{P}^i\text{P})(\text{thione})]$ [12–14]. However, the use of bis(diphenylphosphino)methane (dppm) with its small bite angle resulted in the formation of binuclear copper(I) complexes with bridging dppm [15]. Reacting 1,1,1-tris(diphenylphosphanyl)methyl)ethane (triphos) with copper(I) halides in a 1:1 molar ratio resulted in mononuclear $[\text{CuX}(\text{triphos})]$, which, upon treatment with one equivalent of the potassium thiolate salt of heterocyclic thiones, produced $[\text{Cu}(\kappa^3\text{-triphos})(\kappa^1\text{-thiolate})]$ [16].

Homoleptic and mixed-ligand copper(I) phosphine complexes have been intensively investigated as anticancer agents [17]. For example, tris(hydroxymethyl)phosphine was employed in synthesizing a hydrophilic complex of CuP_4 type, which exhibited greater cytotoxicity than cisplatin [18]. Hadjikakou and co-workers studied the anticancer properties of $[\text{CuCl}(\text{PPh}_3)_3]$ and $[(\text{PPh}_3)\text{Cu}(\mu\text{-Cl})_2\text{Cu}(\text{PPh}_3)_2]$ against leiomyosarcoma cell lines (LMS) and a human breast cancer cell line (MCF-7). Minimum inhibitory concentration (IC_{50}) values were 5 μM all around [19]. Utilizing polypyridyl ligands in synthesizing complexes of the general formula $[\text{Cu}(\text{PPh}_3)_2(\text{N}^i\text{N})]\text{NO}_3$ were achieved, highlighting IC_{50} values against several cancer cell lines in the range 0.32–5.25 μM . Anticancer properties of complexes of the type $[\text{CuX}(\text{P})(\text{N}^i\text{N})]$ were studied intensively by several groups [20–24]. In our group, $[\text{CuBr}(1,10\text{-phenanthroline})(\text{PPh}_3)]$ was screened in vivo against four cancer cell lines and presented cytotoxic effects comparable to cisplatin against MFC-7 and PC3 cancer cell lines [25]. Changing the diimine ligands alters the anticancer properties; optimum cytotoxicity against several cancer cell lines were detected with dipyrido[3,2-a:2',3'-c]phenazine (dppz) ligand and its derivatives [26,27]. However, the thione-containing complexes have received far less attention [28–30]. The current work aimed to examine the potential of Cu(I)-phosphine containing thione ligands as anticancer agents. Specifically, 4,6-dimethylpyrimidine-2-thione was chosen as a ligand in the current work due to the presence of pyrimidines as a core in three nucleobases: cytosine, thymine, and uracil. Moreover, the pyrimidine pharmacophore is present in many antibiotics (e.g., iclaprim), anti-virals (e.g., etravirine), and several other drugs [31]. Several clinically approved anticancer drugs such as fluorouracil, erlotinib, gemcitabine, imatinib, capecitabine, and tegafur contain pyrimidine pharmacophores [32–34]. The synthesis and crystal structure of $\text{CuBr}(\text{PPh}_3)_2(4,6\text{-dimethylpyrimidine-2-thione})$ are described herein. The cytotoxic effects of the complex against two cell lines are also presented and compared to that of cisplatin.

2. Materials and Methods

2.1. Chemicals and Reagents

Solvents (HPLC grade) were used without distillation. Human serum albumin was purchased from Sigma-Aldrich (St. Louis, MO, USA). The synthesis of $\text{CuBr}(\text{PPh}_3)_3$ was achieved as described in the literature, by stirring copper(II) bromide with ca. four molar equivalents of triphenylphosphine in refluxing ethanol under an inert gas atmosphere. The product precipitated after several minutes and was collected by filtration as a white powder [25].

2.2. Instrumentation

High-resolution electrospray ionization (ESI) mass spectra were recorded using an Agilent Q-TOF 6520 instrument (Shelton, CT, USA); all mass spectrometry data are reported as m/z . ^{31}P NMR (242 MHz) spectra were recorded using a Bruker Avance 600 MHz spectrometer equipped with a BBO probe (BrukerBioSpin, Rheinstetten, Germany). The spectra were recorded using previously reported parameters [35]. Absorption spectroscopy was performed using a Genesys-10s UV-VIS spectrophotometer (Thermo Fischer Scientific,

Waltham, MA, USA) and 1 cm path-length quartz cells; bands are reported in the form wavelength (nm).

2.3. Synthesis and Characterization

Equimolar amounts of $\text{CuBr}(\text{PPh}_3)_3$ (0.198 g, 0.214 mmol) and 4,6-dimethylpyrimidien-2-thione ligand (0.030 g, 0.214 mmol) were stirred under nitrogen atmosphere in the appropriate amount of dichloromethane (DCM). The colorless solution turned yellow in a few minutes and was left under stirring for 2 h. The reaction solution was then reduced in volume and 50 mL petroleum spirit (40–60 °C) was added, leading to the precipitation of the product. The product was collected by filtration, washed with diethylether, and dried, affording the complex as a yellow powder (0.149 g, 86%). ^{31}P { ^1H } NMR (CDCl_3 , 600 MHz): -1.56 (s, PPh_3). HR ESI MS: calcd for $[\text{C}_{42}\text{H}_{38}\text{CuN}_2\text{P}_2\text{S}]^+ [\text{M}-\text{Br}]^+$: 727.16269, found: 727.15215. Anal. Calcd for $\text{C}_{42}\text{H}_{38}\text{BrCuN}_2\text{P}_2\text{S}$: C, 62.41; H, 4.74; N, 3.47%; found: C, 62.74; H, 4.86; N, 3.29%.

2.4. Single-Crystal X-ray Diffraction Study

Single crystals of the $[\text{CuBr}(\text{PPh}_3)_2(\text{C}_6\text{H}_8\text{N}_2\text{S})]$ complex were grown by vapor diffusion of hexane into a saturated solution of the compound in dichloromethane at 5 °C. A suitable single crystal was selected and mounted on a Bruker D8 Venture single crystal X-ray diffractometer equipped with Photon II detector (Billerica, MA, USA). The data was collected at 120 K with Mo $\text{K}\alpha$ ($\lambda = 0.71073 \text{ \AA}$) radiation using the Bruker APEX III software package. The crystal structure was solved by the SHELXT [36] structure solution program using Intrinsic Phasing method and refined by least squares method with the SHELXL [37] program implemented in Olex2 [38]. All the non-hydrogen atomic positions were refined anisotropically. The H-atoms were treated as riding, and $U_{\text{iso}}(\text{H})$ values were set at $1.5U_{\text{eq}}(\text{C})$ for methyl and $1.2U_{\text{eq}}(\text{C})$ for aromatic groups. Table 1 summarizes the crystal structure refinement details of the $[\text{CuBr}(\text{C}_{18}\text{H}_{15}\text{P})_2(\text{C}_6\text{H}_8\text{N}_2\text{S})]$.

Table 1. Crystal data and structure refinement for $[\text{CuBr}(\text{C}_{18}\text{H}_{15}\text{P})_2(\text{C}_6\text{H}_8\text{N}_2\text{S})]$.

Empirical formula	$\text{C}_{42}\text{H}_{38}\text{BrCuN}_2\text{P}_2\text{S}$
Formula weight	808.19
Temperature/K	120
Crystal system	Monoclinic
Space group	$P2_1/c$
$a/\text{\AA}$	9.7089(4)
$b/\text{\AA}$	17.8054(6)
$c/\text{\AA}$	21.9786(8)
$\beta/^\circ$	101.040(2)
Volume/ \AA^3	3729.1(2)
Z	4
$\rho_{\text{calc}} \text{ g/cm}^3$	1.440
μ/mm^{-1}	1.832
F(000)	1656.0
Crystal size/ mm^3	$0.355 \times 0.113 \times 0.11$
Radiation/ \AA	Mo $\text{K}\alpha$ ($\lambda = 0.71073$)
Absorption correction	numerical
Index ranges	$-16 \leq h \leq 17 / -31 \leq k \leq 31 / -39 \leq l \leq 39$
Reflections collected	126915
$R_{\text{int}}/R_{\text{sigma}}$	0.0506/0.0426
Data/restraints/parameters	22262/214/532
Goodness-of-fit on F^2	1.015
$R1/wR2$	0.0358/0.0775
Largest diff. peak/hole/ $e \text{ \AA}^{-3}$	0.81/−1.00

2.5. HSA Binding Studies

Human serum albumin (HSA, Product No.: A9511) was purchased from Sigma-Aldrich (St. Louis, MO, USA) and used without further purification. The stock solution of HSA was prepared by using the Tris-HCl/NaCl aqueous buffer system (pH = 7.4). The concentration of HSA (1.2×10^{-5} mol dm⁻³) was measured spectroscopically according to the reported procedure [39]. The solution was titrated with different concentrations of the complex and the ligand in DMSO (the amount of DMSO was maintained at ca. 20% *v/v*). An incubation time of 5 min was used to achieve a homogeneous mixing of both the HSA and the compounds. The changes in the absorption spectra of the solutions were monitored at 295 K.

2.6. Molecular Docking

The crystal structure of the human serum albumin receptor was downloaded from the protein data bank (PDB: 1H9Z) (<http://www.rcsb.org/pdb/home/home.do> accessed on 10 June 2020) [40]. The ligand and its copper complex were sketched in ChemBioOffice Ultra, version 13. All docking studies used the MOE program. HSA (1H9Z) was prepared for the docking study by removing all water and cofactor molecules from the downloaded protein. Then, all invalid charges and broken bonds were corrected, and all hydrogen atoms were added. The parameters and charges were assigned with the MMFF94x force field. After alpha-site spheres were identified using the site finder module of MOE, the two complexes were docked to the same active site of the downloaded compound using the DOCK module of MOE [41,42]. The docking scores in the MOE software were obtained using the London dG scoring function. The highest ten docking scores were used to compare between the two complexes and the co-crystallized reference compound; the values were optimized using two independent refinement methods. The docking results were validated following the reported method [43,44]. The method (the pose selection method) involves re-docking the co-crystallized ligand into the receptor's active site. If the program is able to identify the best pose under a preselected Root Mean Square Deviation (RMSD) value from the known conformation (regularly 1.5 or 2 Å, depending on ligand size), the method is considered "validated". In the current study, pose selection and docking score for R-warfarin (the co-crystallized compound with 1H9Z) were determined; the docking result of the same compound reached a 1.09 Å resolution of the co-crystal structure.

2.7. Anticancer Studies

The cells were supplied by the Egyptian Holding Company for Biological Products and Vaccines (VACSERA) and then kept in the tissue culture unit. The growth of the cells was effected in RPMI-1640 medium, supplemented with 10% heat inactivated FBS, 50 units/mL of penicillin, and 50 mg/mL of streptomycin, and maintained in a humidified atmosphere with 5% carbon dioxide [45,46]. The cells were maintained as monolayer cultures by serial sub-culturing, obtaining cell culture reagents from Lonza (Basel, Switzerland). The anti-tumor activities of the complexes were assessed against OVCAR-3 (ovarian cancer) and HOPE-62 (small cell lung cancer) cell lines.

The sulforhodamine B (SRB) assay method was applied to determine the cytotoxicity, as described in the literature [47]. Exponentially-growing cells were collected using 0.25% Trypsin-EDTA and seeded in 96-well plates at 1000–2000 cells/well in RBMI-1640 supplemented medium. The cells were kept in the medium for 24 h and then they were incubated for 3 days with various concentrations of the copper complexes. Following 3 days of treatment, the cells were fixed with 10% trichloroethanoic acid for 1 h at 4 °C. Wells were stained for 10 min at room temperature with 0.4% SRBC dissolved in 1% acetic acid. The plates were air dried for 24 h and the dye was dissolved in Tris-HCl for 5 min with shaking at 1600 rpm. The optical density (OD) of each well was assessed spectrophotometrically at 564 nm with an ELISA microplate reader (ChroMate-4300, Westport, CT, USA). The minimum inhibitory concentration (IC₅₀) values were calculated from a Boltzmann sigmoidal

concentration response curve using the nonlinear regression fitting models (Graph Pad, Prism Version 9).

3. Results

3.1. Synthesis and Characterization

The synthesis of the complex was achieved by stirring equimolar amounts of $\text{CuBr}(\text{PPh}_3)_3$ and 4,6-dimethylpyrimidine-2-thione in DCM. One phosphine ligand is substituted with the thione, and the driving force of this substitution is the high steric hindrance of the triphenylphosphine as indicated by comparing the X-ray single crystallographic data of the reactant and the product. ^{31}P NMR spectroscopy, elemental analysis, and mass spectrometry were utilized to characterize the compound. In the ^{31}P NMR spectra, the compound shows a sharp singlet signal around -1.5 ppm. The mass spectrum of the compound afforded the peak of $[\text{M}-\text{Br}]^+$ ion. Elemental analysis provided data that are in agreement with the proposed formula. Further confirmation of the structure is provided by the X-ray diffraction crystallographic study.

3.2. Crystal Structure Study

The title compound crystallizes in a monoclinic crystal system with $P2_1/c$ symmetry forming a monomeric complex with four formula units per unit cell ($Z' = 1$). Fractional atomic coordinates, atomic displacement parameters, site occupancy factors, bond lengths, bond angles, and torsion angles are shown in Tables S1–S6 of the Supplementary Materials. Figure 1 shows the molecular structure of $[\text{CuBr}(\text{PPh}_3)_2(\text{C}_6\text{H}_8\text{N}_2\text{S})]$. The geometrical feature of the molecule resembles the parent $[\text{CuBr}(\text{PPh}_3)_3]$ complex and other similar Cu(I) halide complexes with CuXSP_2 cores [14,28,48–50]. The heavily distorted tetrahedral coordination of the copper compound is realized by the S-atom of the –thione, the P-atom of phosphine, and bromo ligands. The bond angles of the CuBrSP_2 tetrahedron varied between 98° and 125° , which notably deviates from the ideal tetrahedral angle (109.4°). The largest deviation of 125° is observed for the P–Cu–P angle, which is more than 6° wider than the P–Cu–P angle (119°) found in $[\text{CuBr}(\text{PPh}_3)_3]$.

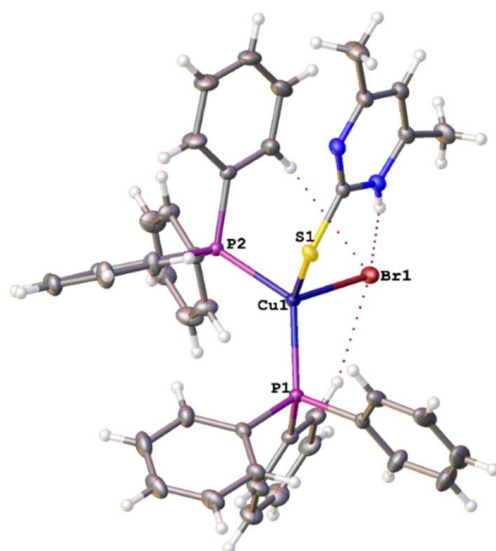


Figure 1. Molecular structure of the $[\text{Cu}(\text{PPh}_3)_2(\text{C}_6\text{H}_8\text{N}_2\text{S})]\text{Br}$ complex. Thermal ellipsoids are drawn at a 50% probability level and the H-atoms are drawn as spheres of arbitrary radii. The intramolecular H-bonds are indicated by red-dotted lines.

This type of tetrahedral distortion is very common in similar complexes [11,28,51] and is mainly attributed to the valence-shell electron-pair repulsion and/or steric imposition of the bulky triphenyl-phosphine group. The distortion of the tetrahedral coordination around an atom can be judged by the so called τ_4 parameter ($\tau_4 = [360 - (\alpha + \beta)]/141$,

where α and β are the largest angles around the central atom), whose value should be equal to one for exact tetrahedral and zero for square planar coordination. For the title compound, $\tau_4 = 0.93$ is slightly higher than the $\tau_4 = 0.90$ of the $[\text{CuBr}(\text{PPh}_3)_3]$ complex, which means that the overall tetrahedral character around the Cu-atom was not substantially altered by the substitution of the PPh_3 group by the -thione ligand. In general, all the interatomic distances are comparable to the corresponding distances reported in identical Cu-complexes [14,28,48–50,52]. In the title compound, the Cu–Br distance (2.5412(2) Å) is slightly longer, while the Cu–P average distance of 2.275 Å became shorter compared to the respective distances (2.497(1) Å and 2.333 Å) observed in the parent compound, which is related to the thione-S donor substitution in the title compound. The intramolecular hydrogen bridges are formed between the amine group ($D_1 = \text{N1}$) of the pyrimidine–thione ligand, the phenyl ring of the phosphine group ($D_2 = \text{C8}$ and C32) and bromine acceptor ($A = \text{Br1}$) with $D \cdots A$ distances $d(D_1 \cdots A) = 3.233(1)$ Å, $d(D_2 \cdots A) = 3.661(9)$ Å, 3.841(2) Å, respectively. These intramolecular H-bonding distances are in the same range as those found in similar structures. The macromolecular feature of the $[\text{CuBr}(\text{PPh}_3)_2(\text{C}_6\text{H}_8\text{N}_2\text{S})]$ complex is established by the intermolecular hydrogen bonding of the bromine acceptor created by symmetry operation $1-x, 1-y, 1-z$ to the methyl group ($D_3 = \text{C42}$) of the pyrimidine–thione ligand forming a centrosymmetric dimer (Figure 2). The intermolecular hydrogen bonding distance of $d(D_3 \cdots A) = 3.879(1)$ Å is slightly longer than the intramolecular hydrogen bridges. This type of structural feature was also observed in the crystal structure of $[\text{CuBr}(\text{PPh}_3)_2(\text{MTUC})]$ [14]. The intra- and intermolecular hydrogen bonding distances are compiled in Table S7 of the SI. No π – π stacking was observed in the crystal structure of the title complex.

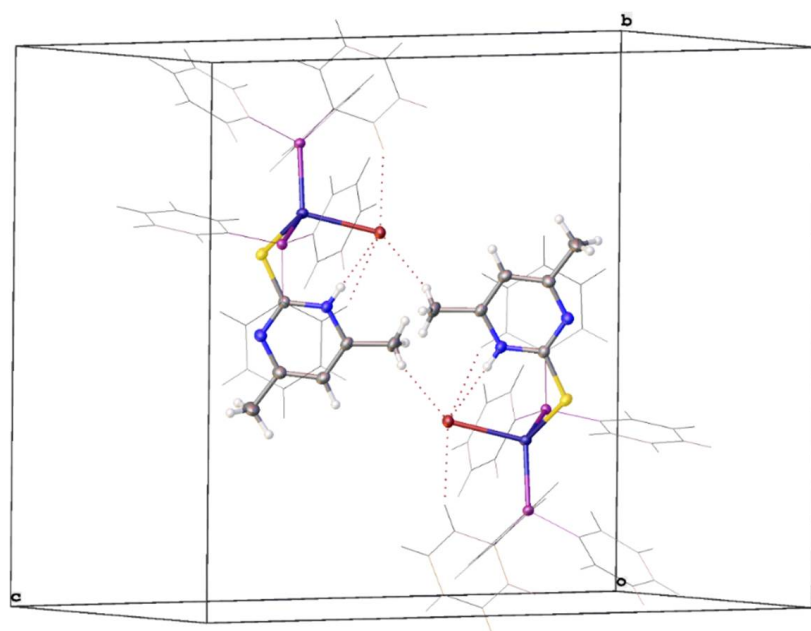


Figure 2. Neighboring molecules of the unit cell form a centrosymmetric dimer via intermolecular hydrogen bonding with $D \cdots A$ distance of 3.879(1) Å. The thermal ellipsoids are drawn at 50% probability level. For clarity, the phenyl rings are drawn as wires and sticks.

3.3. Protein Binding Study

Drug–protein (serum albumin) interactions have been identified as crucial for their delivery [53–56]. Human serum albumin is widely used as a model system for protein folding, aggregation, and drug delivery and it is one of the most abundant proteins present in the blood plasma, comprising about 55% of the blood plasma protein [57–59]. Structural characteristics of HSA have been well investigated. The HSA structure has nearly 580 amino acid residues in one chain, which presumes a solid equilateral triangular shape with sides of ca. 80 Å and depth of ca. 30 Å [60,61]. The structure of HSA (secondary and

tertiary) is comprised of three α -helical domains I, II, and III. Each of these domains consists of two subdomains stabilized by disulfide bonds [60,61]. Subdomain IIA (site I) is of significance in binding with hydrophobic materials, while subdomain IIIA (site II) is involved in a combination of hydrophobic, hydrogen bonding, and electrostatic interactions with the guest molecules [62–64]. Exploring protein–drug binding by UV-vis absorption is a simple but effective technique. The absorption spectrum of HSA features a strong absorption band at 240 nm related to the protein backbone (α -helix structure), and a weak absorption band at 278 nm assigned to the absorption of aromatic amino acids (Trp, Tyr and Phe) [65]. The absorption spectra of HSA was collected in the presence of increasing amounts of the ligand and its copper(I) complex. As illustrated in Figure 3, the two compounds behave differently with the protein. The band intensity of HSA at 240 nm increased significantly with a slight red-shift upon increasing concentrations of the ligand, while the intensity of the band at 278 nm increased with a blue-shift in the absorption maxima. The presence of pronounced changes around 240 nm suggests conformational changes in the α -helix structure of the protein, while changes around 278 nm indicates a strong impact on the microenvironment of the HSA aromatic amino acids by the binding of the ligand (Figure 3). However, the addition of Cu-L into the protein causes weak decreases in the intensities of the absorption band at 240, suggesting that the complex interacts differently from its ligand. The complex slightly affects the α -helix structure of the protein, but insignificantly changes the microenvironment of the HSA aromatic amino acids.

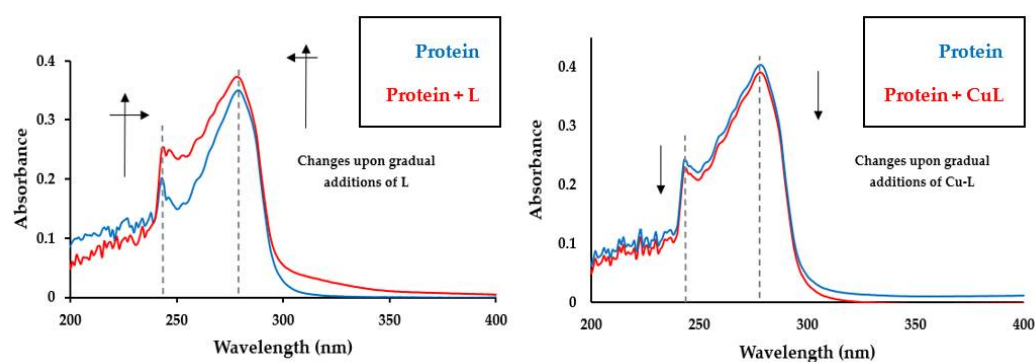


Figure 3. Changes in the absorption spectrum of HSA upon titration with L (left) and Cu-L (right).

3.4. Molecular Docking

Molecular docking is a powerful tool for computer-assisted drug design with the aim to predict a drug's key binding modes with the 3D structure of the biomolecular target. Docking can be utilized to justify experimental results and extract structural–property relationships, which are significant for further optimization [66]. The docking study was conducted to gain insight into the binding sites and the potential interactions of the compounds in the protein microenvironment [67]. The lowest five binding energies of the two forms of the ligand (thiole and thione) and its copper complex were obtained. For the ligand, the docking scores suggest that the thione form has a slightly better docking score than the thiole form. Hence, the thione form will be discussed in detail. The docking results suggest that the thione ligand binds in the pocket between subdomain I B and subdomain II A, forming hydrogen bonding with Gln 196, Lys 199, and Cys 200 (Figure 4) [68]. This explains the strong impact induced by the ligand on the spectrum of the protein (at 240 nm) since cysteine units are responsible for the α -helix structure. The presence of the ligand in this area may allow for hydrophobic interactions with tryptophan (214), phenylalanine (149, 156, 157, 165, 206, and 211), and tyrosine (148, 150, and 161) amino acids available in this area. In contrast, Cu-L has a better binding score toward HSA than that calculated for the ligand (Table 2). The data indicate that Cu-L has a strong preference to bind exclusively to subdomain II A (Figure 4). The complex forms some H-bonding interactions with Lys 199 and Arg 222; there is proximity for Cu-L with any cysteine unit, which explains the small impact of the molecule on the α -helix structure. However, the binding site of Cu-L is

surrounded by several tryptophan, phenylalanine, and tyrosine amino acids, which may allow for weak electrostatic, hydrophobic, and/or van der Waals interactions with Cu-L. The dramatic difference in the binding sites for L and Cu-L rationalize the spectral changes induced by the molecule–protein binding.

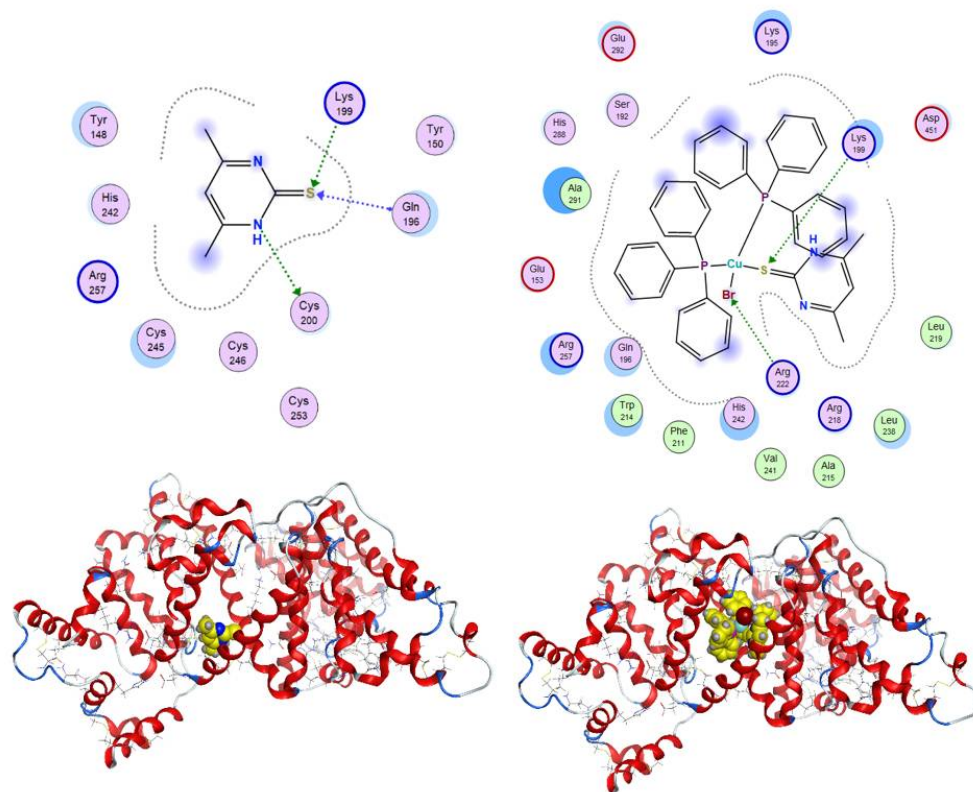


Figure 4. Different interaction domains of L (left) and Cu-L (right) with HSA.

Table 2. Binding scores and interactions of L and Cu-L against HSA as proposed by MOE.

Compound	Binding Domain	Binding Score	Donor → Acceptor
R-warfarin	II A	−6.27	(OH) _{aliph} → His288 Arg257 → (OH) _{aliph}
L	I B/II A	−4.83	(NH) → Cys200 Lys199 → (S) Gln196 → (S)
Cu-L	II A	−8.38	Lys199 → (S) Arg222 → (Br)

3.5. Anticancer Activities

The anticancer properties of L and Cu-L were assessed against ovarian carcinoma (OVCAR-3) and cervical cancer (HeLa) cell lines (see Table 3), as well as rhesus monkey normal kidney epithelial cells (LLC-MK2). The obtained IC₅₀ values against the cancer cell lines for 4,6-dimethylpyrimidine-2-thione ranged from 19.37 to 21.35 μM; coordinating the thione to the CuBr(PPh₃)₂ moiety enhances the anticancer activities, reducing IC₅₀ values by nearly 30%. The minimum inhibitory concentrations for Cu-L against the two cancer cell lines are within a narrow range from that of cisplatin, which does not allow conclusive comparison. L and Cu-L were also examined against the LLC-MK2 cell line as a model to evaluate cytotoxicity for normal cells. The compounds show good selectivity toward cancerous cells, as can be represented by the “selectivity index”. The selectivity index was previously used to measure selective cytotoxic activity [69]. The selectivity index (SI) can be calculated from the ratio of IC₅₀ of the compound on LLC-MK2 to the IC₅₀ of the

compound on a cancer cell line. The selectivity index for L was in the range of 25.6 to 28.2 while it was in the range 43.0 to 49.8 for Cu-L, highlighting the higher selectivity for the copper(I) complex.

Table 3. Anticancer activities of L, Cu-L, and cisplatin in DMSO solutions.

Compound	OVCAR-3 (IC50% in μM)	HeLa (IC50% in μM)	LLC-MK2 (IC50% in μM)
L	21.35 \pm 1.30	19.37 \pm 0.71	>100
Cu-L	15.12 \pm 0.48	13.05 \pm 0.61	>100
cisplatin	11.87 \pm 1.91	11.45 \pm 0.60	>100

4. Conclusions

In the current work, a complex with the formula $\text{CuBr}(\text{PPh}_3)_2(4,6\text{-dimethylpyrimidine-2-thione})$ (Cu-L) was synthesized by stirring $\text{CuBr}(\text{PPh}_3)_3$ and 4,6-dimethylpyrimidine-2-thione in dichloromethane. The crystal structure of Cu-L was obtained, and indicated that the complex adopts a distorted tetrahedral structure. Compared to the parent complex, the Cu-Br distance is slightly longer, while Cu-P bond lengths are shorter. Several intramolecular hydrogen bonds are established, while a centrosymmetric dimer is formed by the intermolecular hydrogen bonding of the bromine acceptor created by symmetry operation $1-x, 1-y, 1-z$ to the methyl group ($D_3 = C42$) of the pyrimidine-thione ligand. The binding of Cu-L and its ligand against HSA was conducted by following the changes in the UV-vis absorption of the protein upon the addition of the compounds; Cu-L binds to HSA differently from its ligand. The ligand seems to affect the α -helix structure while Cu-L has an insignificant impact on the α -helix structure of the HSA protein. The Cu-L binds to the II A domain while L binds between the I B and II A domains, as suggested by docking modelling. Anticancer activities against OVCAR-3 and HeLa cell lines highlighted the significance of the copper center in enhancing the cytotoxic effect. Moreover, Cu-L has more selectivity toward cancer cell lines than the thione ligand. Overall, the current results highlight that complexes of the type CuXP_2S can be explored for accessing new therapeutic agents.

Supplementary Materials: The following are available online at <https://www.mdpi.com/article/10.3390/cryst11060688/s1>, Table S1: Fractional Atomic Coordinates for Cu-L, Table S2: Anisotropic Displacement Parameters for Cu-L, Table S3: Atomic Occupancy for Cu-L, Table S4: Bond Lengths for Cu-L, Table S5: Bond Angles for Cu-L, Table S6: Torsion Angles for Cu-L, Table S7: Hydrogen Bonds for CuL. Crystal data have been deposited at the Cambridge Crystallographic Data Centre and has been assigned the deposition number CCDC 2076663. The data are obtainable free of charge from The Cambridge Crystallographic Data Centre via www.ccdc.cam.ac.uk/structures accessed on 16 June 2021.

Author Contributions: Conceptualization, B.A.B.; Data curation, J.H.A.; Formal analysis, J.H.A., M.H.A., B.D., A.-H.E. and M.J.; Funding acquisition, B.A.B.; Investigation, B.A.B. and M.J.; Methodology, B.D. and A.-H.E.; Project administration, B.A.B.; Resources, M.J. and M.H.A.; Software, M.H.A. and M.A.H.; Supervision, B.A.B.; Visualization, B.D. and M.A.H.; Writing—original draft, B.A.B.; Writing—review & editing, B.A.B. All authors have read and agreed to the published version of the manuscript.

Funding: M.J. would like to express his thanks to KAUST for financial and technical support.

Institutional Review Board Statement: Not applicable.

Informed Consent Statement: Not applicable.

Data Availability Statement: The data presented in this study are available on request from the authors.

Acknowledgments: J.H.A., M.A.H. and B.A.B. would like to express their thanks to KAU for technically supporting this work. M.J. would like to acknowledge King Abdullah University of Science and

Technology (KAUST) for financial support. M.H.A. is very thankful for Taif University researcher support; project number: TURSP/91, Taif University, Taif, Saudi Arabia.

Conflicts of Interest: The authors declare no conflict of interest.

Sample Availability: Not available.

Abbreviations

HSA: Human serum albumin; OVCAR-3: Ovarian carcinoma cancer cell line; HeLa: Cervical cancer cell line; LLC-MK2: rhesus monkey kidney epithelial normal cells.

References

1. Raper, E.S. Complexes of heterocyclic thionates Part 2: Complexes of bridging ligands. *Coord. Chem. Rev.* **1997**, *165*, 475–567. [[CrossRef](#)]
2. Garcia-Vazquez, J.A.; Romero, J.; Sousa, A. Electrochemical synthesis of metallic complexes of bidentate thiolates containing nitrogen as an additional donor atom. *Coord. Chem. Rev.* **1999**, *193*, 691–745. [[CrossRef](#)]
3. Akrivos, P.D. Recent studies in the coordination chemistry of heterocyclic thiones and thionates. *Coord. Chem. Rev.* **2001**, *213*, 181–210. [[CrossRef](#)]
4. Karagiannidis, P.; Aslanidis, P.; Kessissoglou, D.P.; Krebs, B.; Dartmann, M. Mononuclear and binuclear Cu(I) complexes with metal-sulfur ligation. *Inorg. Chim. Acta* **1989**, *156*, 47–56. [[CrossRef](#)]
5. Skoulika, S.; Aubry, A.; Karagiannidis, P.; Aslanidis, P.; Papastefanou, S. New copper(I) chloride complexes with heterocyclic thiones and triphenylphosphine as ligands. Crystal structures of $[\text{Cu}(\text{PPh}_3)_2(\text{bzimth}_2)\text{Cl} \cdot \text{CH}_3\text{COCH}_3$ and $[\text{Cu}(\text{PPh}_3)_2(\text{nbzimth}_2)\text{Cl}]$. *Inorg. Chim. Acta* **1991**, *183*, 207–211. [[CrossRef](#)]
6. Batsala, G.K.; Dokorou, V.; Kourkoumelis, N.; Manos, M.J.; Tasiopoulos, A.J.; Mavromoustakos, T.; Simčić, M.; Golič-Grdadolnik, S.; Hadjikakou, S.K. Copper(I)/(II) or silver(I) ions towards 2-mercaptopyrimidine: An exploration of a chemical variability with possible biological implication. *Inorg. Chim. Acta* **2012**, *382*, 146–157. [[CrossRef](#)]
7. Anastasiadou, D.; Psomas, G.; Lalia-Kantouri, M.; Hatzidimitriou, A.G.; Aslanidis, P. Copper(I) halide complexes of 2,2,5,5-tetramethyl-imidazolidine-4-thione: Synthesis, structures, luminescence, thermal stability and interaction with DNA. *Mater. Sci. Eng. C* **2016**, *68*, 241–250. [[CrossRef](#)]
8. Hadjikakou, S.K.; Aslanidis, P.; Karagiannidis, P.; Mentzafos, D.; Terzis, A. Synthesis and photolysis of mixed copper(I) complexes with thiones and tri-*p*-tolylphosphine or triphenylphosphine; X-ray crystal structure of bis[copper(I)(1,3-thiazolidine-2-thione)(tri-*p*-tolylphosphine)chloride]. *Polyhedron* **1991**, *10*, 935–940. [[CrossRef](#)]
9. Hadjikakou, S.K.; Aslanidis, P.; Akrivos, P.D.; Karagiannidis, P.; Kojic-Prodic, B.; Luic, M. Study of mixed ligand copper(I) complexes with tri-*m*-tolyl-phosphine (tmtpp) and heterocyclic thiones. Crystal structures of bis[μ -S(benzimidazole-2-thione)(tmtpp)copper(I) chloride] and bis[μ -Br(thiazolidine-2-thione)(tmtpp)copper(I)]. *Inorg. Chim. Acta* **1992**, *197*, 31–38. [[CrossRef](#)]
10. Hadjikakou, S.K.; Aslanidis, P.; Karagiannidis, P.; Aubry, A.; Skoulika, S. Copper(I) complexes with tri-*o*-tolylphosphine and heterocyclic thione ligands. Crystal structures of [(pyrimidine-2-thione)(tri-*o*-tolylphosphine)copper(I) chloride] and [(pyridine-2-thione)(tri-*o*-tolylphosphine)copper(I) iodide]. *Inorg. Chim. Acta* **1992**, *193*, 129–135. [[CrossRef](#)]
11. Walia, S.; Kaur, S.; Kaur, J.; Sandhu, A.K.; Lobana, T.S.; Hundal, G.; Jasinski, J.P. Synthesis, Spectroscopy, and Structures of Mono- and Dinuclear Copper(I) Halide Complexes with 1,3-Imidazolidine-2-thiones. *Z. Anorg. Allg. Chem.* **2015**, *641*, 1728–1736. [[CrossRef](#)]
12. Aslanidis, P.; Cox, P.J.; Divanidis, S.; Tsepis, A.C. Copper(I) Halide Complexes with 1,3-Propanebis(diphenylphosphine) and Heterocyclic Thione Ligands: Crystal and Electronic Structures (DFT) of $[\text{CuCl}(\text{pymtH})(\text{dppp})]$, $[\text{CuBr}(\text{pymtH})(\text{dppp})]$, and $[\text{Cu}(\mu\text{-I})(\text{dppp})_2]$. *Inorg. Chem.* **2002**, *41*, 6875–6886. [[CrossRef](#)] [[PubMed](#)]
13. Aslanidis, P.; Cox, P.J.; Divanidis, S.; Karagiannidis, P. Copper(I) halide complexes from cis-1,2-bis(diphenylphosphino) ethylene and some heterocyclic thiones. *Inorg. Chim. Acta* **2004**, *357*, 1063–1076. [[CrossRef](#)]
14. Cox, P.J.; Kaltzoglou, A.; Aslanidis, P. Copper(I) halide chelates of the wide bite angle diphosphane xantphos: Crystal structures of $[\text{CuBr}(\text{xantphos})(\text{dmpymtH})]$ and $[\text{CuI}(\text{xantphos})(\text{imdtH}_2)] \cdot \text{CH}_3\text{CN}$. *Inorg. Chim. Acta* **2006**, *359*, 3183–3190. [[CrossRef](#)]
15. Aslanidis, P.; Cox, P.J.; Tsaliki, P. Copper(I) halide complexes with 2,2'-bis(diphenylphosphano)-1,1'-binaphthyl (rac-binap) and heterocyclic thiones. Racemic compounds in chiral and achiral crystal space groups. *Polyhedron* **2008**, *27*, 3029–3035. [[CrossRef](#)]
16. Rodríguez, A.; Sousa-Pedrares, A.; García-Vázquez, J.A.; Romero, J.; Sousa, A. Synthesis and Structural Characterization of Copper(I), Silver(I) and Gold(I) Complexes with Pyrimidine-2-thionato Ligands and their Adducts with Phosphanes. *Eur. J. Inorg. Chem.* **2011**, *2011*, 3403–3413. [[CrossRef](#)]
17. Tisato, F.; Porchia, M.; Santini, C.; Gandin, V.; Marzano, C. Ch 3—Phosphine-copper(I) complexes as anticancer agents: Design, synthesis, and physicochemical characterization. Part I. In *Copper(I) Chemistry of Phosphines, Functionalized Phosphines and Phosphorus Heterocycles*; Balakrishna, M.S., Ed.; Elsevier: Amsterdam, The Netherlands, 2019; pp. 61–82.
18. Marzano, C.; Gandin, V.; Pellei, M.; Colavito, D.; Papini, G.; Lobbia, G.G.; Giudice, E.D.; Porchia, M.; Tisato, F.; Santini, C. In vitro antitumor activity of the water soluble copper (I) complexes bearing the tris (hydroxymethyl) phosphine ligand. *J. Med. Chem.* **2008**, *51*, 798–808. [[CrossRef](#)]

19. Lazarou, K.; Bednarz, B.; Kubicki, M.; Verginadis, I.I.; Charalabopoulos, K.; Kourkoumelis, N.; Hadjikakou, S.K. Structural, photolysis and biological studies of the bis (μ 2-chloro)-tris (triphenylphosphine)-di-copper (I) and chloro-tris (triphenylphosphine)-copper (I) complexes. Study of copper (I)–copper (I) interactions. *Inorg. Chim. Acta* **2010**, *363*, 763–772. [[CrossRef](#)]
20. Porchia, M.; Dolmella, A.; Gandin, V.; Marzano, C.; Pellei, M.; Peruzzo, V.; Refosco, F.; Santini, C.; Tisato, F. Neutral and charged phosphine/scorpionate copper (I) complexes: Effects of ligand assembly on their antiproliferative activity. *Eur. J. Med. Chem.* **2013**, *59*, 218–226. [[CrossRef](#)]
21. Gandin, V.; Tisatom, F.; Dolmella, A.; Pellei, M.; Santini, C.; Giorgetti, M.; Marzano, C.; Porchia, M. In vitro and in vivo anticancer activity of copper (I) complexes with homoscorpionate tridentate tris (pyrazolyl) borate and auxiliary monodentate phosphine ligands. *J. Med. Chem.* **2014**, *57*, 4745–4760. [[CrossRef](#)]
22. Komarnicka, U.K.; Starosta, R.; Kyziol, A.; Jezowska-Bojczuk, M. Copper (I) complexes with phosphine derived from sparfloxacin. Part I—structures, spectroscopic properties and cytotoxicity. *Dalton Trans.* **2015**, *44*, 12688–12699. [[CrossRef](#)]
23. Komarnicka, U.K.; Starosta, R.; Plotek, M.; de Almeida, R.F.M.; Jezowska-Bojczuk, M.; Kyziol, A. Copper (I) complexes with phosphine derived from sparfloxacin. Part II: A first insight into the cytotoxic action mode. *Dalton Trans.* **2016**, *45*, 5052–5063. [[CrossRef](#)]
24. Komarnicka, U.K.; Starosta, R.; Kyziol, A.; Plotek, M.; Puchalska, M.; Jezowska-Bojczuk, M. New copper (I) complexes bearing lomefloxacin motif: Spectroscopic properties, in vitro cytotoxicity and interactions with DNA and human serum albumin. *J. Inorg. Biochem.* **2016**, *165*, 25–35. [[CrossRef](#)] [[PubMed](#)]
25. Mashat, K.; Babgi, B.A.; Hussien, M.A.; Arshad, M.N.; Abdellatif, M. Synthesis, structures, DNA-binding and anticancer activities of some copper(I)-phosphine complexes. *Polyhedron* **2019**, *158*, 164–172. [[CrossRef](#)]
26. Babgi, B.A.; Mashat, K.H.; Abdellatif, M.H.; Arshad, M.N.; Alzahrani, K.A.; Asiri, A.M.; Du, J.; Humphrey, M.G.; Hussien, M.A. Synthesis, structures, DNA-binding, cytotoxicity and molecular docking of CuBr (PPh₃)(diimine). *Polyhedron* **2020**, *192*, 114847. [[CrossRef](#)]
27. Alsaedi, S.; Babgi, B.A.; Abdellatif, M.H.; Arshad, M.N.; Emwas, A.; Jaremko, M.; Humphrey, M.G.; Asiri, A.M.; Hussein, M.A. DNA-Binding and Cytotoxicity of Copper(I) Complexes Con-taining Functionalized Dipyridylphenazine Ligands. *Pharmaceutics* **2021**, *13*, 764–1–764-13. [[CrossRef](#)] [[PubMed](#)]
28. Aslanidis, P.; Cox, P.J.; Kapetangiannis, K.; Tsipis, A.C. Structural and Spectroscopic Properties of New Copper(I) Complexes with 1,1,1-Tris(diphenylphosphanylmethyl)ethane and Heterocyclic Thiolates. *Eur. J. Inorg. Chem.* **2008**, *2008*, 5029–5037. [[CrossRef](#)]
29. Khan, A.; Jasinski, J.P.; Smoleaski, V.A.; Paul, K.; Singh, G.; Sharma, R. Synthesis, structure and cytotoxicity evaluation of complexes of N¹-substituted-isatin-3-thiosemicarbazone with copper(I) halides. *Inorg. Chim. Acta* **2016**, *449*, 119–126. [[CrossRef](#)]
30. Papazoglou, I.; Cox, P.J.; Hatzidimitriou, A.G.; Kokotidou, C.; Choli-Papadopoulou, T.; Aslanidis, P. Copper(I) halide complexes of 5-carboxy-2-thiouracil: Synthesis, structure and in vitro cytotoxicity. *Eur. J. Med. Chem.* **2014**, *78*, 383–391. [[CrossRef](#)]
31. Sahu, M.; Siddiqui, N. A review on biological importance of pyrimidines in the new era. *Int. J. Pharm. Pharm. Sci.* **2016**, *8*, 8–21.
32. Martin, D.S.; Bertino, J.R.; Koutcher, J.A. ATP Depletion + Pyrimidine Depletion Can Markedly Enhance Cancer Therapy: Fresh Insight for a New Approach. *Cancer Res.* **2000**, *60*, 6776–6783.
33. Farguay, A.M.; Habib, N.S.; Ismail, K.A.; Hassan, A.M.M.; Sarg, M.T.M. Synthesis, Biological Evaluation and Molecular Docking Studies of Some Pyrimidine Derivatives. *Eur. J. Med. Chem.* **2013**, *66*, 276–295. [[CrossRef](#)] [[PubMed](#)]
34. Helwa, A.A.; Gedawy, E.M.; Abou-Seri, S.M.; Taher, A.T.; El-Ansary, A.K. Synthesis and bioactivity evaluation of new pyrimidinone-5-carbonitriles as potential anticancer and antimicrobial agents. *Res. Chem. Intermed.* **2018**, *44*, 2685–2702. [[CrossRef](#)]
35. Al-Masri, H.T.; Emwas, A.M.; Al-Talla, Z.A.; Alkordi, M.H. Synthesis and Characterization of New N-(Diphenylphosphino)-Naphthylamine Chalcogenides: X-Ray Structures of (1-NHC₁₀H₇)P(Se)Ph₂ and Ph₂P(S)OP(S)Ph₂. *Phosphorus Sulfur Silicon Relat. Elem.* **2012**, *187*, 1082–1090. [[CrossRef](#)]
36. Sheldrick, G. SHELXT—Integrated space-group and crystal-structure determination. *Acta Cryst. Sect. A Found. Adv.* **2015**, *71*, 3–8. [[CrossRef](#)]
37. Sheldrick, G. Crystal structure refinement with SHELXL. *Acta Cryst. Sect. C Struct. Chem.* **2015**, *71*, 3–8. [[CrossRef](#)] [[PubMed](#)]
38. Dolomanov, O.V.; Bourhis, L.J.; Gildea, R.J.; Howard, J.A.K.; Puschmann, H. OLEX2: A complete structure solution, refinement and analysis program. *J. Appl. Cryst.* **2009**, *42*, 339–341. [[CrossRef](#)]
39. Hoefelschweiger, B.K.; Duerkop, A.; Wolfbeis, O.S. Novel type of general protein assay using a chromogenic and fluorogenic amine-reactive probe. *Anal. Biochem.* **2005**, *344*, 122–129. [[CrossRef](#)]
40. Petitpas, I.; Bhattacharya, A.A.; Twine, S.; East, M.; Curryi, S. Crystal structure analysis of warfarin binding to human serum albumin: Anatomy of drug site I. *J. Biol. Chem.* **2001**, *276*, 22804–22809. [[CrossRef](#)]
41. Al-Khathami, N.D.; Al-Rashdi, K.S.; Babgi, B.A.; Hussien, M.A.; Arshad, M.N.; Eltayeb, N.E.; Elsilik, S.E.; Lasri, J.; Basaleh, A.S.; Al-Jahdali, M. Spectroscopic and biological properties of platinum complexes derived from 2-pyridyl Schiff bases. *J. Saudi Chem. Soc.* **2019**, *23*, 903–915. [[CrossRef](#)]
42. Abdel-Rhman, M.H.; Hussien, M.A.; Mahmoud, H.M.; Hosny, N.M. Synthesis, characterization, molecular docking and cytotoxicity studies on N-benzyl-2-isonicotinoylhydrazine-1-carbothioamide and its metal complexes. *J. Mol. Struct.* **2019**, *1196*, 417–428. [[CrossRef](#)]
43. Cole, J.C.; Murray, C.W.; Nissink, J.W.; Taylor, R.D.; Taylor, R. Comparing protein-ligand docking programs is difficult. *Proteins* **2005**, *60*, 325–332. [[CrossRef](#)]
44. Jain, A.N. Bias, reporting, and sharing: Computational evaluations of docking methods. *J. Comput. Aided Mol. Des.* **2008**, *22*, 201–212. [[CrossRef](#)]
45. Muanza, D.N.; Kim, B.W.; Euler, K.L.; Williams, L. Antibacterial and Antifungal Activities of Nine Medicinal Plants from Zaire. *Int. J. Pharm.* **1994**, *32*, 337–345. [[CrossRef](#)]

46. Pezzuto, J.M.; Che, C.-T.; McPherson, D.D.; Zhu, J.-P.; Topcu, G.; Erdelmeier, C.A.J.; Cordell, G.A. DNA as an Affinity Probe Useful in the Detection and Isolation of Biologically Active Natural Products. *J. Nat. Prod.* **1991**, *54*, 1522–1530. [[CrossRef](#)] [[PubMed](#)]
47. Skehan, P.; Storeng, R.; Scudiero, D.; Monks, A.; McMahon, J.; Vistica, D.; Warren, J.; Bokesch, H.; Kenney, S.; Boyd, M. New Colorimetric Cytotoxicity Assay for Anticancer-Drug Screening. *J. Natl. Cancer Inst.* **1990**, *82*, 1107–1112. [[CrossRef](#)] [[PubMed](#)]
48. Lobana, T.S.; Sandhu, A.K.; Sultana, R.; Castineiras, A.; Butcher, R.J.; Jasinski, J.P. Coordination variability of Cu^I in multidonor heterocyclic thioamides: Synthesis, crystal structures, luminescent properties and ESI-mass studies of complexes. *RSC Adv.* **2014**, *4*, 30511–30522. [[CrossRef](#)]
49. Anastasiadou, D.; Psomas, G.; Kalogiannis, S.; Geromichalos, G.; Hatzidimitriou, A.G.; Aslanidis, P. Bi- and trinuclear copper(I) compounds of 2,2,5,5-tetramethylimidazolidine-4-thione and 1,2-bis(diphenylphosphano)ethane: Synthesis, crystal structures, in vitro and in silico study of antibacterial activity and interaction with DNA and albumins. *J. Inorg. Biochem.* **2019**, 110750. [[CrossRef](#)] [[PubMed](#)]
50. Charalampou, D.C.; Kourkoumelis, N.; Karanestora, S.; Hadjiarapoglou, L.P.; Dokorou, V.; Skoulika, S.; Owczarzak, A.; Kubicki, M.; Hadjikakou, S.K. Mono- and Binuclear Copper(I) Complexes of Thionucleotide Analogues and Their Catalytic Activity on the Synthesis of Dihydrofurans. *Inorg. Chem.* **2014**, *53*, 8322–8333. [[CrossRef](#)] [[PubMed](#)]
51. Koutsari, A.; Karasmani, F.; Kapetanaki, E.; Zainuddin, D.I.; Hatzidimitriou, A.G.; Angaridis, P.; Aslanidis, P. Luminescent thione/phosphane mixed-ligand copper(I) complexes: The effect of thione on structural properties. *Inorg. Chim. Acta* **2017**, *458*, 138–145. [[CrossRef](#)]
52. Lecomte, C.; Skoulika, S.; Aslanidis, P.; Karagiannidis, P.; Papastefanou, S. Copper(I) bromide complexes with heterocyclic thiones and triphenylphosphine as ligands. The X-ray crystal structure of copper(I) pyrimidine-2-thione bis (triphenylphosphine) bromide [Cu(PPh₃)₂(PymtH)Br]. *Polyhedron* **1989**, *8*, 1103–1109. [[CrossRef](#)]
53. Ascone, I.; Messori, L.; Casini, A.; Gabbiani, C.; Balerna, A.; Dell'Unto, F.; Castellano, A.C. Exploiting Soft and Hard X-Ray Absorption Spectroscopy to Characterize Metallodrug/Protein Interactions: The Binding of [trans-RuCl₄(Im)(dimethylsulfoxide)][ImH] (Im = imidazole) to Bovine Serum Albumin. *Inorg. Chem.* **2008**, *47*, 8629–8634. [[CrossRef](#)] [[PubMed](#)]
54. Groessl, M.; Terenghi, M.; Casini, A.; Elviri, L.; Lobinski, R.; Dyson, P.J. Reactivity of anticancer metallodrugs with serum proteins: New insights from size exclusion chromatography-ICP-MS and ESI-MS. *J. Anal. At. Spectrom.* **2010**, *25*, 305–313. [[CrossRef](#)] [[PubMed](#)]
55. Shmykov, A.Y.; Filippov, V.N.; Foteeva, L.S.; Keppler, B.K.; Timerbaev, A.R. Toward high-throughput monitoring of metallodrug-protein interaction using capillary electrophoresis in chemically modified capillaries. *Anal. Biochem.* **2008**, *379*, 216–218. [[CrossRef](#)] [[PubMed](#)]
56. Timerbaev, A.R.; Hartinger, C.G.; Aleksenko, S.S.; Keppler, B.K. Interactions of Antitumor Metallodrugs with Serum Proteins: Advances in Characterization Using Modern Analytical Methodology. *Chem. Rev.* **2006**, *106*, 2224–2248. [[CrossRef](#)] [[PubMed](#)]
57. Gibellini, D.; Vitone, F.; Schiavone, P.; Ponti, C.; Placa, M.L.; Re, M.C. Quantitative detection of human immunodeficiency virus type 1 (HIV-1) proviral DNA in peripheral blood mononuclear cells by SYBR green real-time PCR technique. *J. Clin. Virol.* **2004**, *29*, 282. [[CrossRef](#)]
58. Lakowicz, J.R. *Principles of Fluorescence Spectroscopy*, 3rd ed.; Springer: New York, NY, USA, 2006.
59. Al-Harhi, S.; Lachowicz, J.I.; Nowakowski, M.E.; Jaremko, M.; Jaremko, Ł. Towards the functional high-resolution coordination chemistry of blood plasma human serum albumin. *J. Inorg. Biochem.* **2019**, *198*, 110716. [[CrossRef](#)]
60. Helms, M.K.; Petersen, C.E.; Bhagavan, N.V.; Jameson, D.M. Time-resolved fluorescence studies on site-directed mutants of human serum albumin. *FEBS Lett.* **1997**, *408*, 67–70. [[CrossRef](#)]
61. El-Kemary, M.; Gil, M.; Douhal, A. Relaxation Dynamics of Piroxicam Structures within Human Serum Albumin Protein. *J. Med. Chem.* **2007**, *50*, 2896–2902. [[CrossRef](#)]
62. He, X.M.; Carter, D.C. Atomic structure and chemistry of human serum albumin. *Nature* **1992**, *358*, 209–215. [[CrossRef](#)]
63. Lhiaubet-Vallet, V.; Sarabia, Z.; Boscá, F.; Miranda, M.A. Human Serum Albumin-Mediated Stereodifferentiation in the Triplet State Behavior of (S)- and (R)-Carprofen. *J. Am. Chem. Soc.* **2004**, *126*, 9538–9539. [[CrossRef](#)] [[PubMed](#)]
64. Yeggoni, D.P.; Gokara, M.; Manidhar, D.M.; Rachamalla, A.; Nakka, S.; Reddy, C.S.; Subramanyam, R. Binding and Molecular Dynamics Studies of 7-Hydroxycoumarin Derivatives with Human Serum Albumin and Its Pharmacological Importance. *Mol. Pharm.* **2014**, *11*, 1117–1131. [[CrossRef](#)] [[PubMed](#)]
65. Shahabadi, N.; Kashanian, S.; Shalmashi, K.; Roshanfekr, H. DNA Interaction with PtCl₂(LL) (LL = Chelating Diamine Ligand: N,N-Dimethyltrimethylendiamine) Complex. *Appl. Biochem. Biotechnol.* **2009**, *158*, 1–10. [[CrossRef](#)] [[PubMed](#)]
66. Morris, G.M.; Lim-Wilby, M. Molecular docking. In *Molecular Modeling of Proteins*; Humana Press: Totowa, NJ, USA, 2008; Volume 443, pp. 365–382.
67. Bhattacharya, B.; Nakka, S.; Guruprasad, L.; Samanta, A. Interaction of Bovine Serum Albumin with Dipolar Molecules: Fluorescence and Molecular Docking Studies. *J. Phys. Chem. B* **2009**, *113*, 2143–2150. [[CrossRef](#)] [[PubMed](#)]
68. Guizado, T.R.C.; Louro, S.R.W.; Anteneodo, C. Dynamics of heme complexed with human serum albumin: A theoretical approach. *Eur. Biophys. J.* **2012**, *41*, 1033–1042. [[CrossRef](#)]
69. Badisa, R.B.; Darling-Reed, S.F.; Joseph, P.; Cooperwood, J.S.; Latinwo, L.M.; Goodman, C.B. Selective Cytotoxic Activities of Two Novel Synthetic Drugs on Human Breast Carcinoma MCF-7 Cells. *Anticancer Res.* **2009**, *29*, 2993–2996.